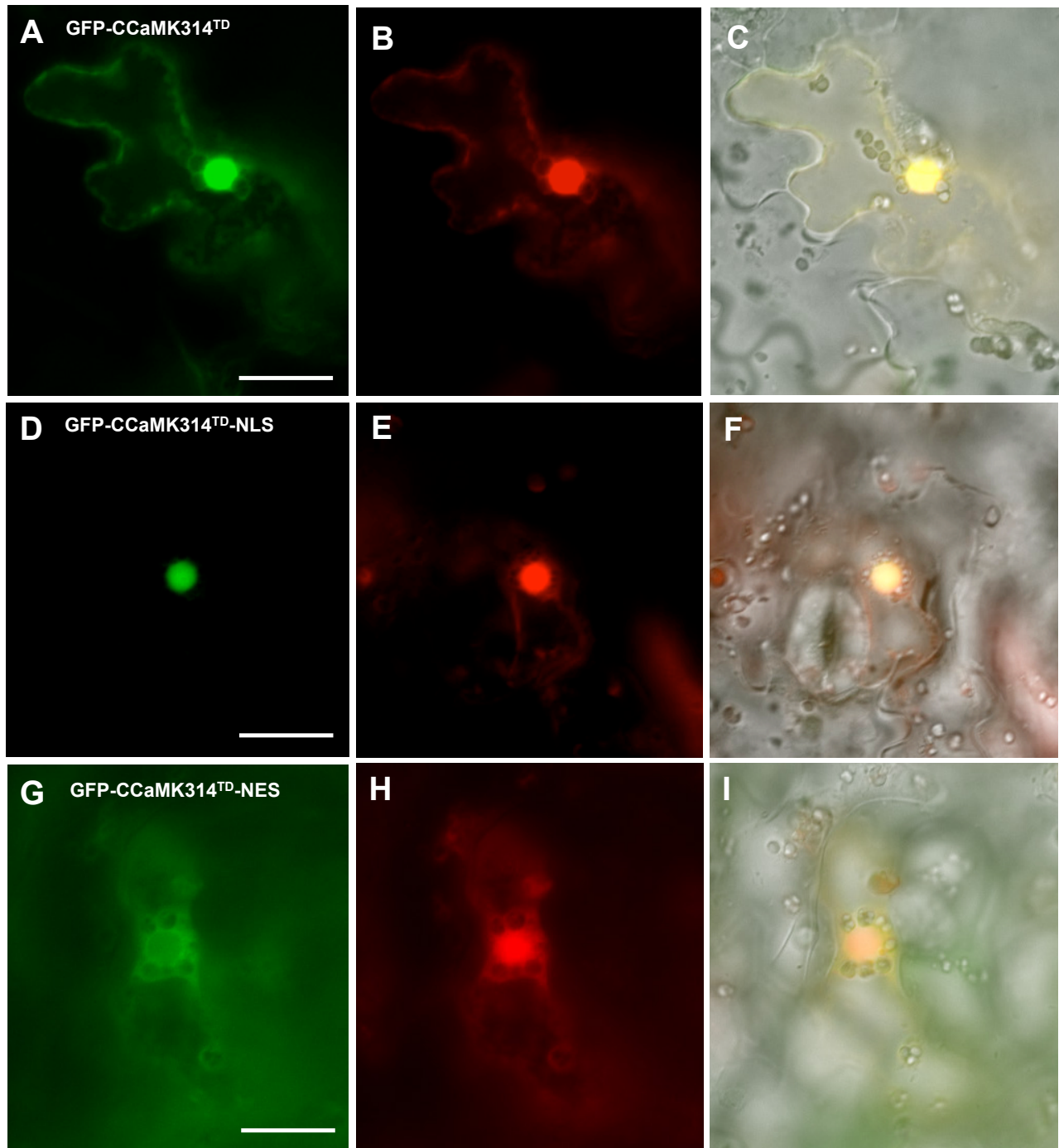


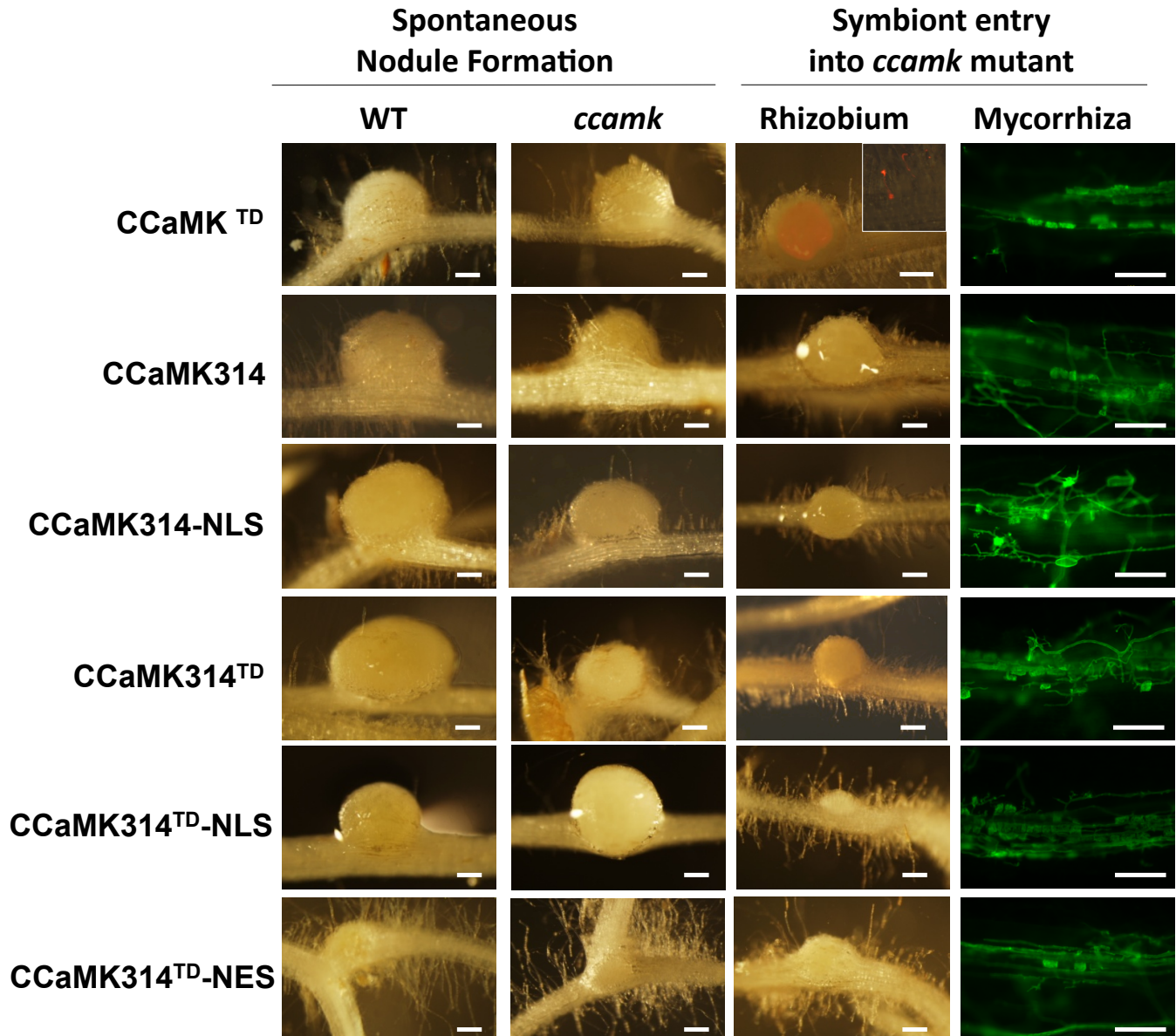
Supplemental Figure 1. Wild-type CCaMK and GOF-CCaMK variants used in this study.

Full-length CCaMK and its T265D substitution, CCaMK^{TD} was constructed by Banba et al. (2008). The truncated GOF-CCaMK variants were constructed in this study. NLS; nuclear localization signal, NES; nuclear export signal.



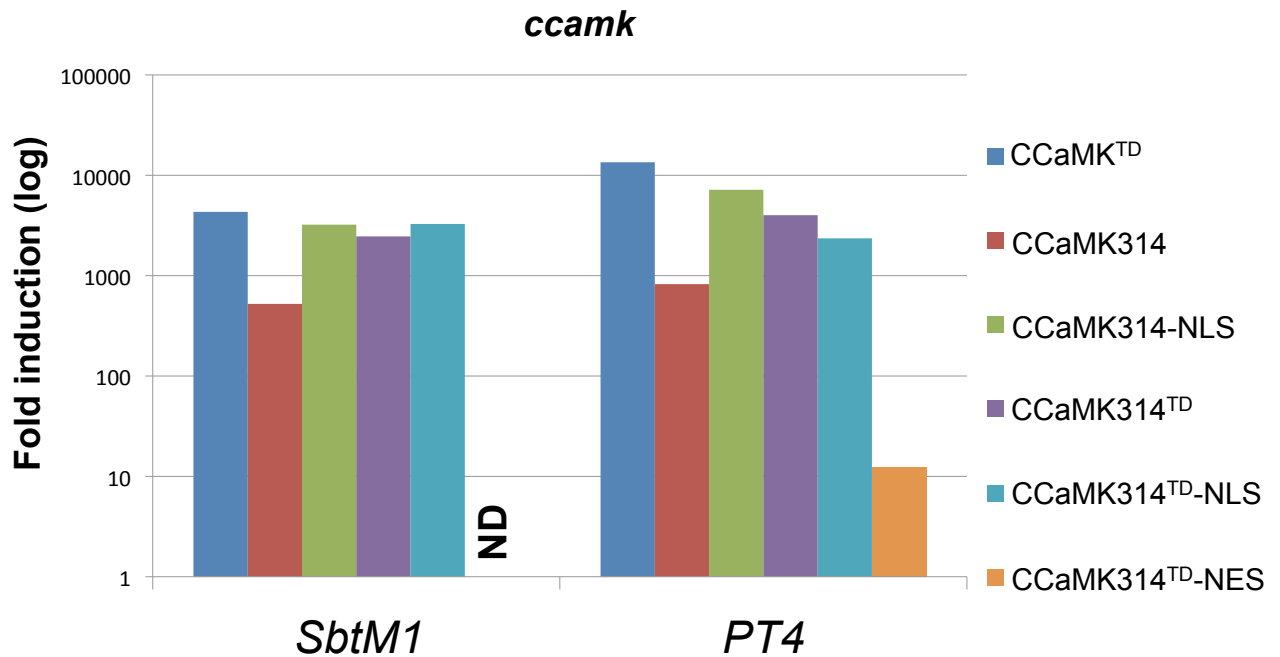
Supplemental Figure 2. Localization of GOF-CCaMK.

GOF-CCaMK variants fused with GFP were introduced with free DsRed into *N. benthamiana* leaf epidermal cells by *Agrobacterium*-mediated infiltration. The transgenic cells carrying GFP-CCaMK314^{TD} (A, B, C), GFP-CCaMK314^{TD}-NLS (D, E, F) and GFP-CCaMK314^{TD}-NES (G, H, I) were observed two days after infiltration. The GFP (A, D, G) and DsRed (B, E, H) fluorescence images were merged with a bright field image (C, F, I). Bars = 25 μ m.



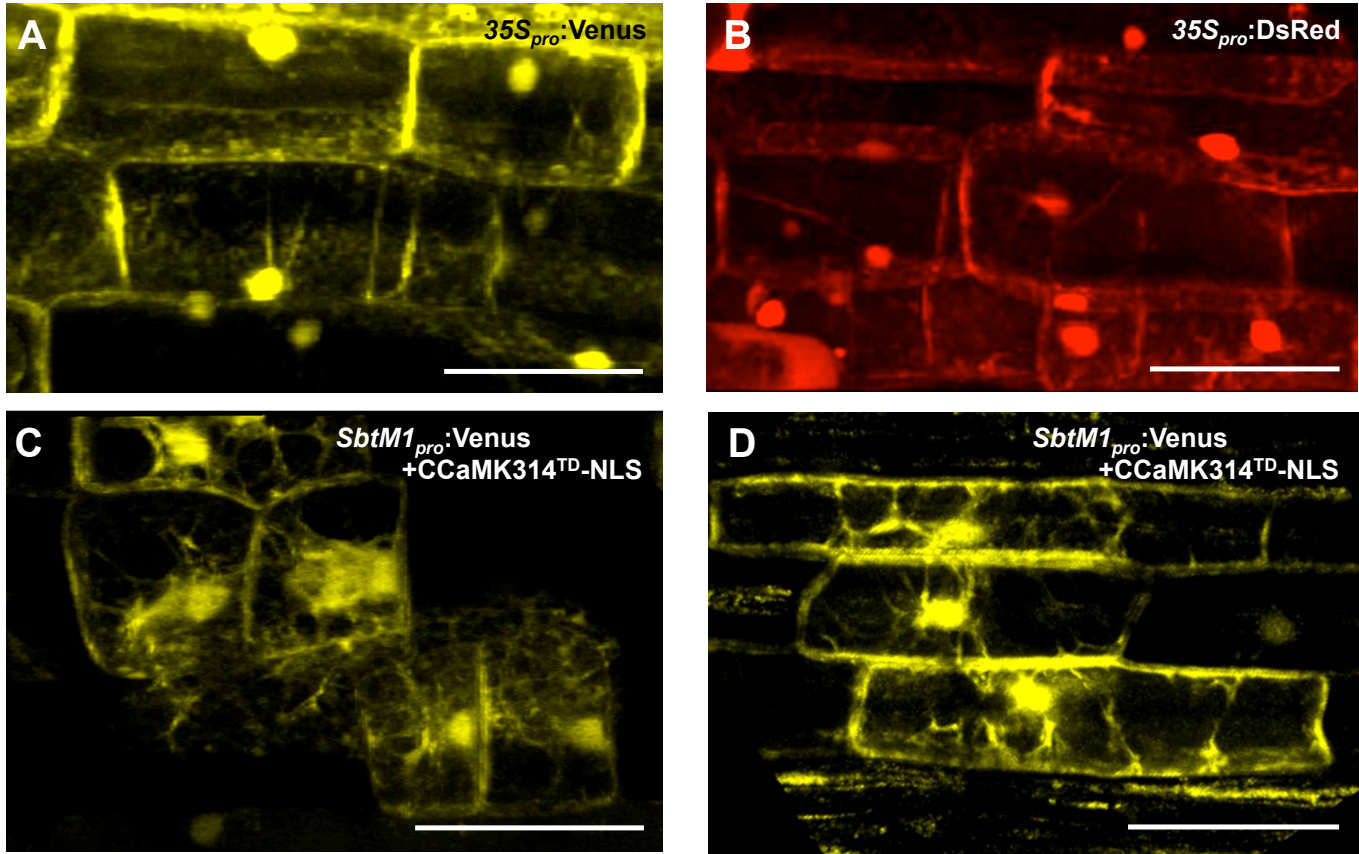
Supplemental Figure 3. SPN formation and complementation of *ccamk* mutants by GOF-CCaMK.

GOF-CCaMK variants were introduced into WT and *ccamk* mutants in order to examine SPN formation and complementation of RNS or AMS phenotype. The SPN formation in WT and *ccamk* mutants was observed in 4 week-old transgenic hairy roots. SPN formation was observed in hairy roots carrying all kinds of GOF-CCaMK. Complementation of rhizobial or AM fungal infection was examined at 4 or 2 weeks after inoculation respectively. Infection thread formation and entry of rhizobia into nodules were detected using *M. loti* expressing DsRed. Only full-length CCaMK^{TD} showed entry of rhizobia. The rest of GOF-CCaMK variants develop nodules without bacterial entry. AM fungi were visualized with WGA Alexa Fluor 488. AM colonization as well as formation of arbuscules and vesicles was observed in hairy roots carrying all kinds of GOF-CCaMK. Bars = 200 μ m.



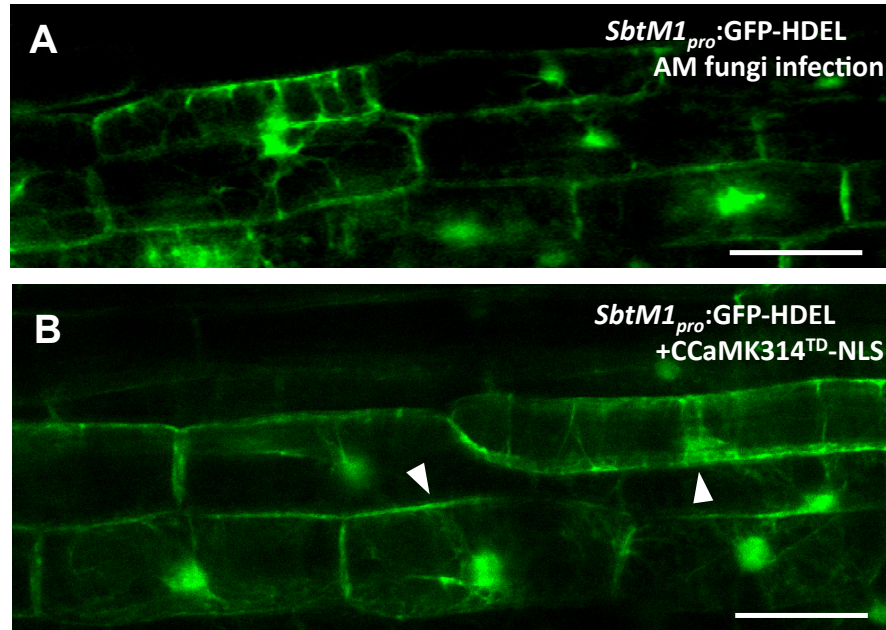
Supplemental Figure 4. Activation of AMS-induced genes by GOF-CCaMK in *ccamk* mutants.

Induction of *SbtM1* and *PT4* were detected in hairy roots carrying a series of GOF-CCaMK variants at 2 weeks after AM fungi inoculation. Fold induction levels were calculated compared with the transgenic hairy roots carrying a control vector (p35S-GFP) (fold value = 1) and shown in logarithmic scale. ND; Not detected.



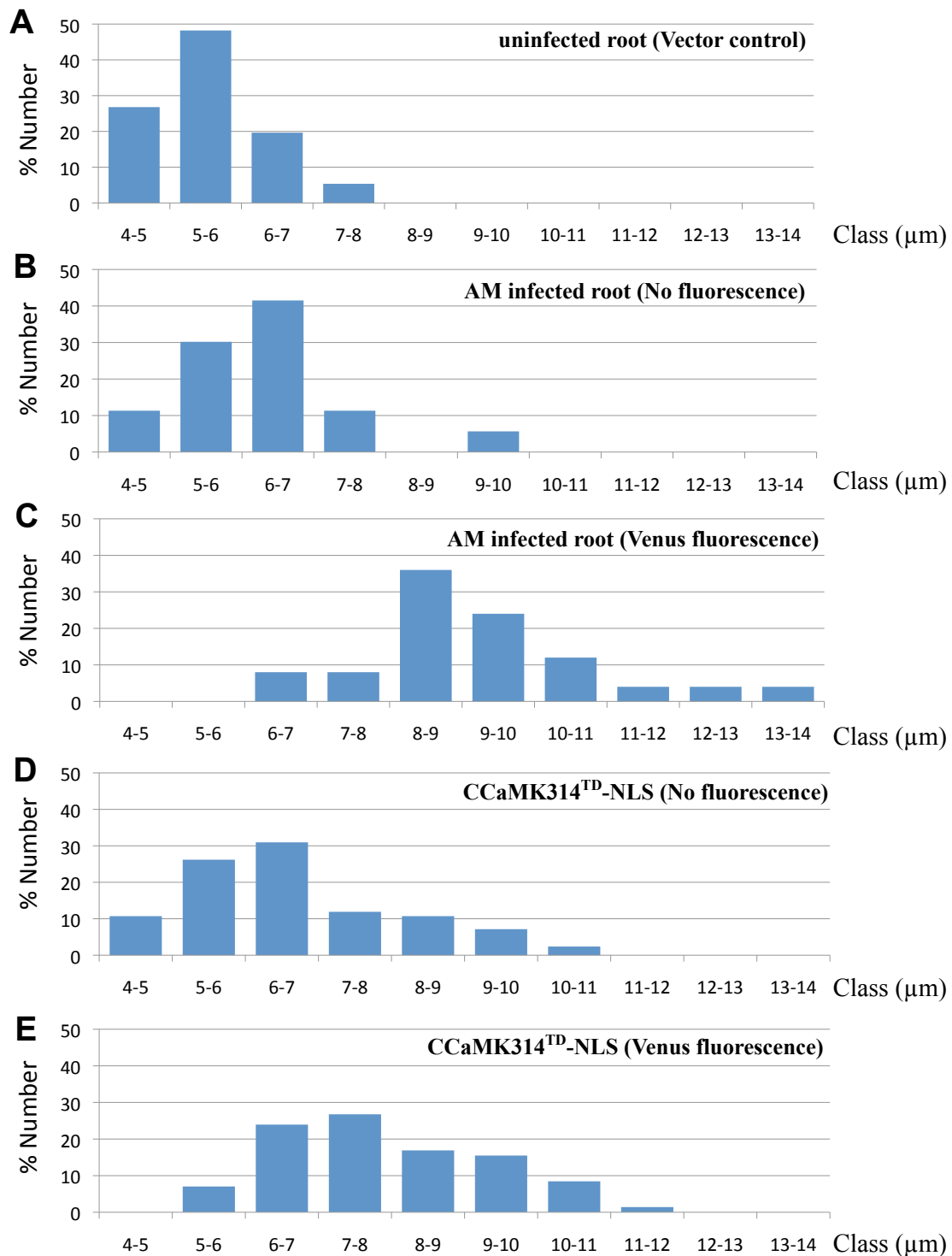
Supplemental Figure 5. Transvacuolar strands and PPA-like structures induced by GOF-CCaMK.

A stack images of transvacuolar strands (A-B) visualized with $35S_{pro}$:Venus (A) or co-transformation maker; $35S_{pro}$:DsRed (B), and those of the PPA-like structures visualized with $SbtM1_{pro}$:Venus (C, D). Transvacuolar strands were observed as thin threads of cytoplasm (A). Cells neighboring to those showing the PPA-like structures had fewer and thinner cytoplasmic bridges corresponding to normal transvacuolar strands in the similar cell types (B). Densely developed cytoplasmic bridges were observed in $SbtM1_{pro}$:Venus expressing cells (C). The image corresponds to Figure 4C-E. Various sizes of cells showed the PPA-like structures (D). Conditions of observation were as same as Figure 4. Bars = 50 μ m.



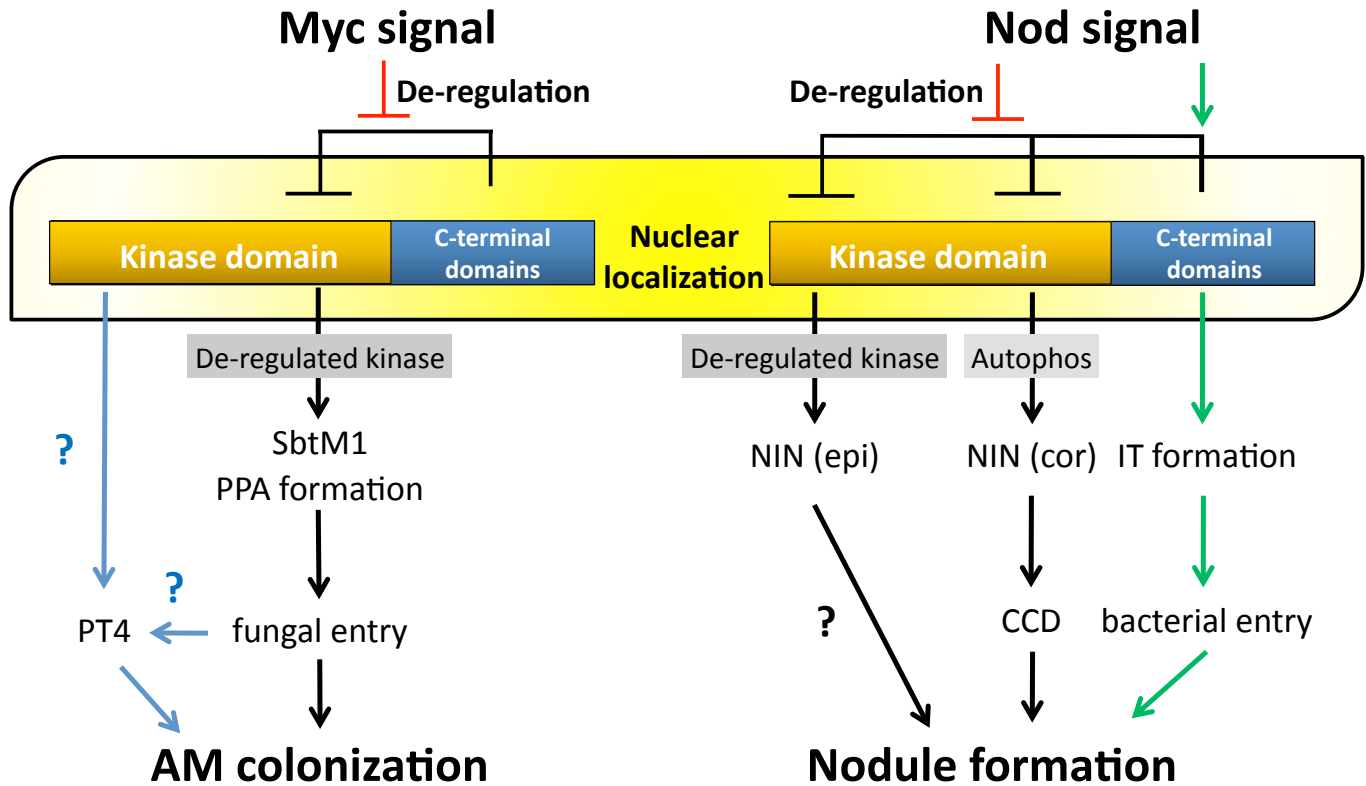
Supplemental Figure 6. PPA-like structures visualized by ER-retained GFP.

Transgenic roots carrying *SbtM1_{pro}:GFP-HDEL* showed development of ER in cortical cells 2 weeks after AM fungi inoculation (A). Development of ER and the PPA-like structures were induced by CCaMK314^{TD}-NLS (B). Tubular-like ERs, a characteristic structure of the PPA were observed in some cells expressing GFP-HDEL (arrowheads). Bar = 50 μ m.



Supplemental Figure 7. Histograms of nuclear sizes in cortical cells.

Nuclear sizes of uninfected roots (A), AM fungi infected roots (B, C) and roots carrying CCaMK^{TD}-NLS (D, E) were measured after DAPI staining. Venus fluorescent cells in AM fungi infected roots (C) and those in roots carrying CCaMK^{TD}-NLS (E) contained enlarged nuclei. Cells without fluorescence in the corresponding roots (B, D) showed similar distribution to the uninfected roots carrying a control vector (*35S_{pro}:Venus*) (A). These graphs are drawn using individual values summarized in Table 2.



Supplemental Figure 8. Model of CCaMK-regulated AMS and RNS signaling.

Myc signal modifies conformation of CCaMK and de-regulates the kinase activity in a similar manner to kinase-only GOF-CCaMK. This type of activation/de-regulation triggers AMS-induced gene expression and fungal entry. Direct involvement of CCaMK in induction of *PT4* expression is not clear yet. In RNS, signaling through CCaMK is more complex than that in AMS. Cortical (cor) *NIN* expression is induced by autophosphorylated CCaMK (represented by full-length CCaMK^{TD}). De-regulated CCaMK (represented by kinase-only CCaMK) is required for the epidermal (epi) *NIN* expression. Furthermore, bacterial entry through infection threads (ITs) requires presence of the regulatory (C-terminal) domains. The nuclear localization of CCaMK is required for the proper function of CCaMK.